Explosive volcanic eruptions can act as carbon sinks

Delmelle, Pierre; Biasse, Sébastien; Paque, Mathilde; Lobet, Benjamin

How to cite

DELMELLE, Pierre et al. Explosive volcanic eruptions can act as carbon sinks. In: Nature communications, 2025, vol. 16, n° 1. doi: 10.1038/s41467-025-59692-4

This publication URL: https://archive-ouverte.unige.ch/unige:184925
Publication DOI: 10.1038/s41467-025-59692-4

nature communications

Article

https://doi.org/10.1038/s41467-025-59692-4

Explosive volcanic eruptions can act as carbon sinks

Received: 18 August 2024

Accepted: 30 April 2025

Published online: 08 May 2025

Check for updates

Pierre Delmelle[1] ✉, Sébastien Biass[2], Mathilde Paque[1] & Benjamin Lobet[1]

Volcanic soils, covering only ~1% of the Earth's land, store over 5% of the global soil organic C stock. The frequent burial of these soils by tephra fallout from explosive volcanic eruptions is a critical but poorly quantified C storage process in soils from volcanically active regions. Using field measurements, we demonstrate that single eruptions can bury substantial amounts of stable organic carbon in soils. We develop a modelling framework and estimate that, in Ecuador alone, at least 1.1 Pg C has been stored in volcanic soils repeatedly affected by tephra deposition during the Holocene. This stock of tephra-buried soil organic carbon exceeds the cumulative CO_2 emissions from the source eruptions. Here, we show that explosive volcanism, through the repeated burial of organic C in volcanic soils, acts as a significant regional C sink over time, ultimately averaging to net C-negative events.

Tephra emissions associated with explosive volcanic eruptions serve as the primary substrate for volcanic soil formation. Volcanic soils exhibit a unique capacity for SOC accumulation, particularly during the first few thousand years of pedogenesis[1,2]. This property is attributed to abundant reactive surfaces, the creation of organo-mineral associations and the development of microaggregation which protect SOC from microbial decomposition[3–5]. In addition, being co-located with Late Pleistocene and Holocene terrestrial volcanoes[2], organic C-rich volcanic soils are prone to repeated and widespread burial by tephra fallout from explosive eruptions. A tephra deposit just a few tens of centimetres thick, forming in a few hours to a few days, can halt the development of pre-existing soils while providing fresh parent material for new pedogenesis. The recurrence of this process, occurring at intervals ranging from a few years to several thousand years, is responsible for the formation of multi-layered volcanic soils, typically featuring several subsurface horizons with high SOC content[2,6]. Importantly, due to unfavourable environmental conditions for decomposers and a lower accessibility to decomposers and limited input of fresh organic matter[5,7–10], the buried SOC can be stable over millennial timescales[5,7,11,12]. The combination of high SOC accumulation rates and repeated burial results in volcanic soils generally containing more organic C than other mineral soil types[1,2].

Although it has long been suggested that volcanic soil burial by tephra increases SOC content[2], the causal impact of explosive eruptions on SOC stocks in volcanically active regions has still not been unequivocally demonstrated[2,12,13]. The difficulty lies in quantitatively accounting for both the magnitude-frequency relationship of volcanic explosive eruptions and the accumulation of SOC over time in soils repeatedly affected by tephra deposition. Measuring total C stocks in volcanic soils limits our understanding of how explosive volcanism affects SOC storage over time, as stocks give only a single value of C inventory in a system for a sampling year. Here, we hypothesise that repeated tephra fallout from explosive eruptions plays a major role in the build-up of SOC stocks in volcanically active regions by sequestering substantial amounts of organic C in volcanic soils.

The accumulation of SOC in soils ultimately sequesters atmospheric C that was initially captured by plants through photosynthesis. In the soil-plant system, some C is diverted from the short-term (daily to annual timescale) photosynthesis–respiration cycle into inorganic C phases during chemical weathering of silicates present in the soil parent material. However, in the first few thousand years of soil formation, organic C accumulation typically far exceeds CO_2 removal by silicate weathering[14]. Therefore, we posit that the burial of organic C by tephra in volcanic soils is the primary mechanism through which an explosive eruption may act as a C sink, that is, when more C is sequestered in the buried soils than is released into the atmosphere as magmatic CO_2 during the eruption.

Based on field data, we first demonstrate that soil burial by tephra fallout from single eruptions can lead to significant storage of stable organic C in the subsurface soils. We then develop a modelling

[1]Environmental Sciences, Earth and Life Institute, UCLouvain, Louvain-la-Neuve, Belgium. [2]Department of Earth Sciences, University of Geneva, Geneva, Switzerland. ✉e-mail: pierre.delmelle@uclouvain.be

framework to quantify the spatio-temporal accumulation of the tephra-buried SOC stock in a region repeatedly affected by explosive eruptions (Fig. 1) and compare this stored C to the total mass of magmatic CO_2 emissions directly associated with these eruptions.

Results

SOC stock buried by tephra from a single explosive eruption

We estimated the SOC stock stored in the soil intercalated between the tephra deposits from the last two eruptions of the Atacazo-Ninahuilca Volcanic Complex, located in the Western Cordillera of Ecuador, 10 km southwest of Quito (Fig. 2). These Plinian events (Volcanic Explosive Index (VEI)[15] 5), known as N5 (4400 ± 35 BP) and N6 (2270 ± 15 BP), produced ≥ 1 km^3 of dacitic tephra (ref. 16). We sampled 35 soil profiles at altitudes ranging from 1273 to 3772 m within a ~ 1560 km^2 area corresponding to the 10-cm contour of the N6 tephra deposit (Fig. 2; "Methods"). The SOC content (C_{SOC}) is significantly lower ($P < 0.001$) in the soil buried by the N6 tephra fallout (C_{SOC} = 10–36 g C kg^{-1}) compared to the surface soil (C_{SOC} = 23–68 g C kg^{-1}) formed from this deposit (Supplementary Table 1). Both soils developed from tephra of the same composition (dacite), over comparable time periods of surface exposures of ~2100 and 2270 years[16], respectively, and under similar climatic conditions; accordingly, it is reasonable to assume that SOC would have accumulated at roughly the same rate[17,18]. However, human-induced variations in vegetation cover may have occurred locally over time, which could partly account for the difference in soil C_{SOC} between the buried and surface soils. Alternatively, a more likely explanation is partial loss of SOC after burial due to mineralisation of its most labile fraction[7,9]. The remaining stock of the tephra-buried SOC is stable on a millennial time scale, as suggested by C-14 ages ranging from 1800 ± 60 to 2365 ± 55 yr (Supplementary Table 2).

We found that SOC density (in g C m^{-2}) in soils buried by the N6 tephra is predictable based on altitude (Supplementary Fig. 1), consistent with the idea that temperature and precipitation (which typically decreases and increases with altitude, respectively) are the primary factors driving SOC decomposition and storage[17–19]. By applying this relationship to a 30-m digital elevation model[20], we estimated the SOC stock buried by the N6 tephra ~2340 years ago, yielding a total mass of ~18 (3–33) Tg C (Methods). This is a conservative result because soil burial by tephra can occur for deposits thinner than 40 cm, hence covering a larger surface area and increasing the buried SOC stock. Additionally, tephra redistribution following deposition may increase further the surface area impacted by burial. We also calculated that the magmatic CO_2 emitted into the atmosphere by the N6 eruption amounted to 5.7–8.7 (median = 7.1) Tg of C (Methods). Thus, the SOC stock buried by the N6 tephra is up to ~6 times larger than the mass of magmatic C released by the source eruption. Therefore, we contend that soil burial by tephra can turn an explosive eruption into a negative-C emission event.

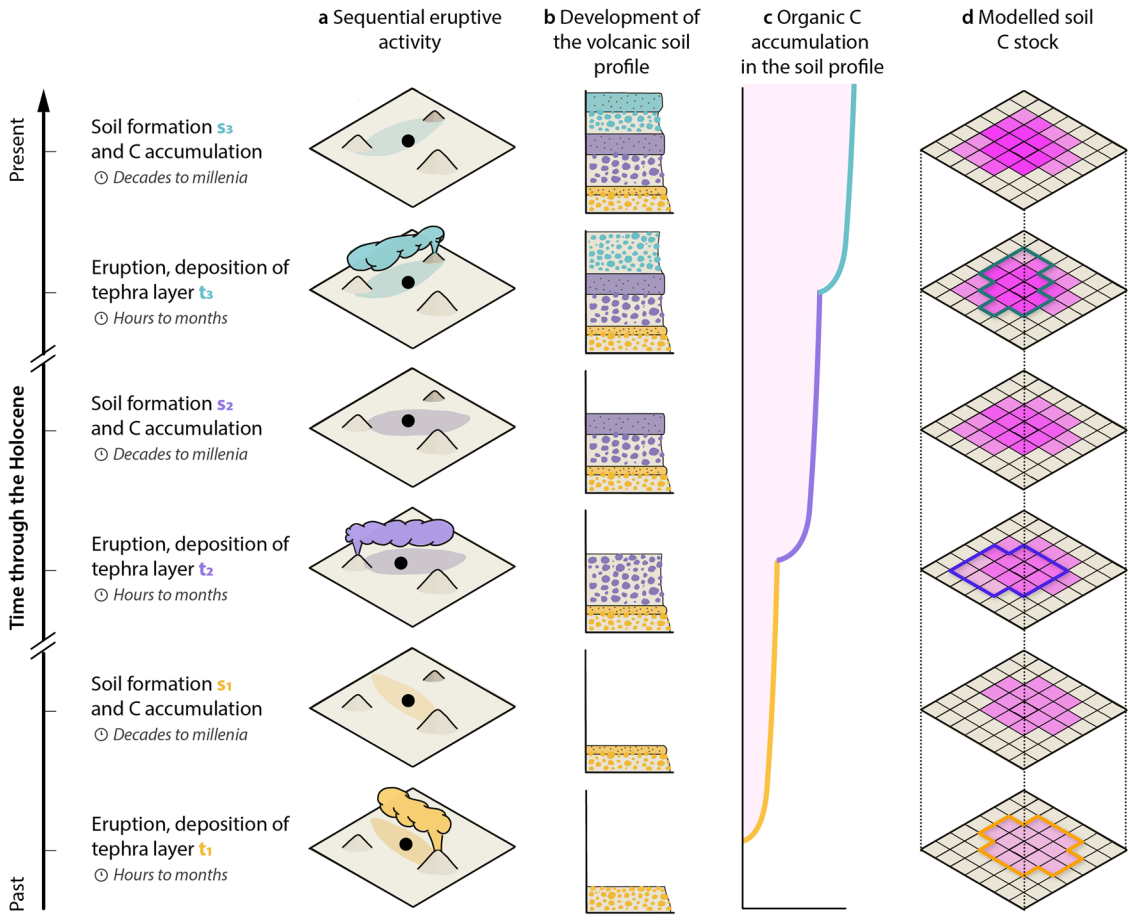

Fig. 1 | Conceptual modelling framework for quantifying SOC accumulation in soils repeatedly buried by tephra deposits from explosive eruptions over time. **a** Schematic representation of a region repeatedly affected by tephra fallout. Multiple volcanoes can produce tephra deposits of which distribution depends on eruptive and wind conditions. **b** Development of a multi-layered volcanic soil at the location indicated by the black dot in (**a**). Soil formation is reset each time a tephra fallout buries the pre-existing soil formed from the previous tephra deposit. The letters "t" and "s" stand for tephra layer and soil, respectively. **c** Accumulation of organic C in the soil buried by a tephra deposit. **d** Conceptual implementation of the modelling framework to quantify the spatio-temporal evolution of the SOC stock. The coloured contours represent the extent of the modelled tephra deposit that buries the pre-existing volcanic soil, and deeper shades of pink represent an increase in the SOC stock.

https://doi.org/10.1038/s41467-025-59692-4

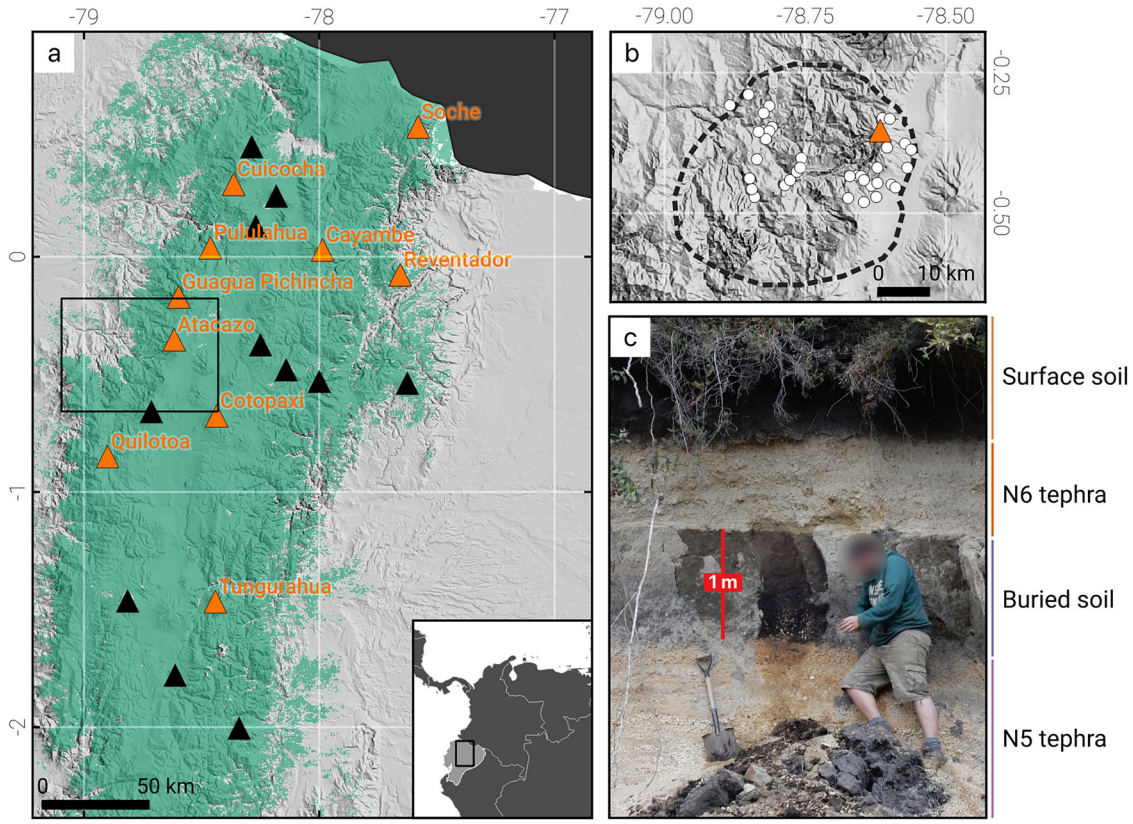

Fig. 2 | Location map of the Atacazo-Ninahuilca case study and photo of a multi-layered volcanic soil. a Ecuadorian volcanoes (triangles) active during the Holocene. Volcanoes with eruptions of VEI ≥ 4 are displayed as orange triangles. The green-shaded area represents the extent of volcanic soils[21]. **b** Zoom on the rectangle in (**a**) showing the location of the 35 sampled volcanic soil profiles used to estimate the SOC stock buried by the tephra from the N6 (2270 ± 15 BP) eruption of Atacazo-Ninahuilca volcano. The dashed contour is the 10 cm isopach of the N6 tephra and the orange triangle indicates the volcano location. **c** Typical volcanic soil profile with the surface soil formed from the N6 tephra deposit and the soil buried by this tephra and which formed from the older N5 tephra deposit (4400 ± 35 BP). Background topography is from NASA shuttle radar topography mission[20].

SOC accumulation in soils repeatedly buried by tephra over time

To quantitatively assess how much SOC can be sequestered over time in a region repeatedly affected by tephra fallout from explosive volcanoes, we developed a modelling framework to predict the spatio-temporal distribution of tephra deposits on the ground and the subsequent accumulation of SOC in the buried soils (Fig. 1 and Supplementary Fig. 2). Additionally, the model enables estimation of the magmatic CO_2 released by the explosive eruptions within a given time interval. We applied our model ('Methods') using the Ecuadorian segment of the Andean volcanic belt, ~30% of which is covered with volcanic soils formed from tephra[21,22] (Fig. 2). We considered only eruptions of VEI 4, 5 and 6. This region has experienced 42 eruptions with a VEI ≥ 4 originating from ten volcanoes during the Holocene[23].

The spatial distribution of tephra accumulation on the ground was calculated using a probabilistic modelling approach[24] ('Methods'). To account for uncertainties, we considered tephra accumulations associated with 10, 50 and 90% exceedance probabilities. We also evaluated the minimum tephra thickness necessary for effective soil burial, testing three values of 10, 30 and 50 cm. Using the eruptive record of the ten identified volcanoes and correcting for record completeness, we estimated for continental Ecuador an average recurrence interval of eruptions of VEI 4, 5 and 6 and generated 1000 synthetic eruption catalogues simulating the Holocene eruptive history. Our modelling framework can be conceptualised as a three-dimensional matrix with a spatial grid covering the Ecuadorian Andes at a resolution of 1 km and a temporal resolution of 1 month (Fig. 1d). For each time step of a given catalogue, we first tested if an eruption occurs, in which case a VEI and a source volcano were sampled based on the eruption record.

Our model provides constraints, at any location in Ecuador, on the time between two consecutive eruptions that generated tephra deposits thick enough to bury surface soil. Where burial occurs, this time interval represents the duration of accumulation of organic C in the new surface soil that forms from the tephra deposit (Fig. 1b and c). Volcanic soils exhibit a unique capacity for SOC storage, with ~31 kg C m^{-2} on average, which is second only to organic soils[1] (Histosols). According to refs. 12,25,26, the rate of organic C accretion in volcanic soils decreases as a power function of soil age, regardless of the climate zone. We refitted this power law with additional data points and described uncertainties (Supplementary Fig. 4). Using this relationship, we estimated the cumulative amount of organic C stored in volcanic soils across Ecuador, with each grid cell's SOC stock being the result of 1000 synthetic eruptive catalogues for the Holocene. To account for the potential loss of labile organic C after tephra burial[7,9], we adopted a cautious approach and divided the computed SOC stock by two. This is consistent with our field observations at Atacazo-Ninahuilca and a modelling study[9], which shows that the burial of topsoil can lead to the preservation of up to half of the initial C_{SOC}.

Explosive eruptions drive SOC storage and act as C sinks

Based on the median time-dependent SOC accrual rate and assuming a 50% probability of soil burial by 30 cm of tephra, our model indicates that ~1.1 Pg of organic C has accumulated in soils covered by tephra from Holocene eruptions in Ecuador (Fig. 3). When considering the 10th and 90th percentile of the SOC accumulation rate-time regression model (Supplementary Fig. 4), the estimated tephra-buried SOC stock values are lower (~0.3 Pg) and slightly higher (~1.2 Pg), respectively

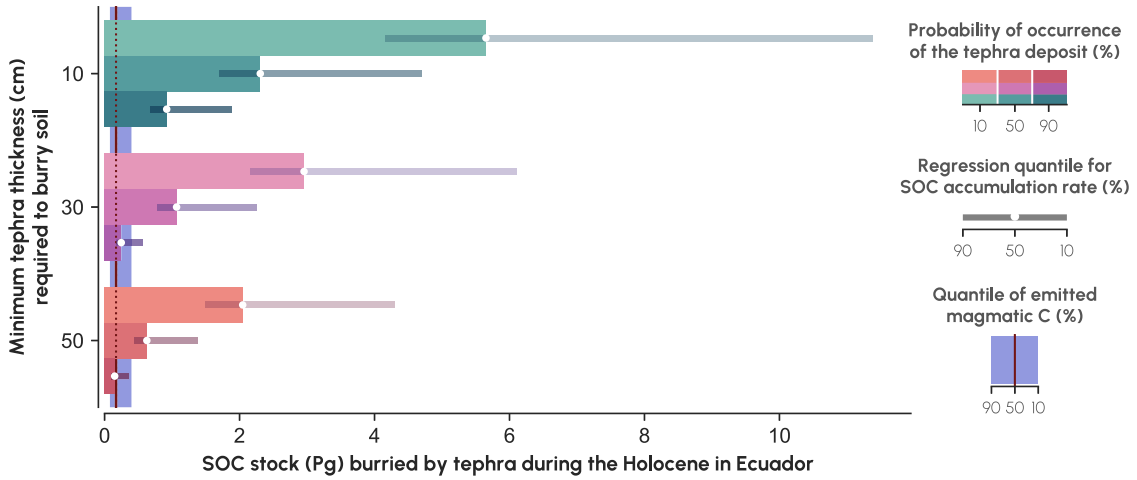

Fig. 3 | Cumulative SOC stock in volcanic soils repeatedly buried by tephra from VEI ≥ 4 eruptions in Ecuador during the Holocene. The SOC stock estimates (horizontal bars) are based on the 10th, 50th and 90th regression quantiles of the SOC accumulation rate-time relationship (Supplementary Fig. 4) and three probabilities (30, 50, and 90%) of occurrence of tephra deposits with thicknesses of 10, 30 and 50 cm. The 10th, 50th and 90th percentiles of the cumulative mass of magmatic C emitted are also shown. The total mass of magmatic C emitted explosively over the same period is shown for comparison (vertical blue bar).

(Fig. 3 and Supplementary Table 6). Higher SOC storage in soils is predicted for conditions that decrease the minimum tephra thickness and/or tephra isomass probability, and vice versa. Due to conditions that are unfavourable for microbial respiration[7,8], the residence time of buried SOC stocks is likely to be on the order of centuries to millennia, as also already indicated by our C-14 analyses at Atacazo-Ninahuilca (Supplementary Table 2) and other studies[5,11,27–29].

Our results unambiguously show that, in volcanically active regions, the combination of rapid organic C accumulation during volcanic soil accretion and recurrent soil burial by tephra deposits leads to substantial storage at depth of organic C. For Ecuador, the SOC stock in volcanic soils covered repeatedly by tephra during the Holocene may make up as much as one-third of the country's total stock (~3.2 Pg of C to a depth of 1 metre beneath the surface[30]). Over a similar period, tephra fallout in Ecuador has led to the sequestration of as much organic C in soils as the regional-scale Bignell loess deposition episode that could have buried ~0.7–2.7 Pg C in a paleosoil (the Brady soil in Nebraska, USA) 10,500–9,000 years ago[31]. However, comparing SOC stocks on a per square kilometre basis reveals that Ecuadorian explosive volcanism may have resulted in ~4.5 times greater organic C storage (Supplementary Methods), highlighting recurrent tephra deposition as a particularly efficient geological process for sequestrating C at depth. Our analysis reinforces the idea that soil burial mediated by volcanic materials constitutes a significant contribution to the total soil C stock[13,32,33].

Repeated tephra fallout events during the Holocene may have led to the storage of ~1.9 Mg C km^{-2} yr^{-1}, or ~11 Tg C yr^{-1}, in Ecuadorian soils. This estimate, while slightly lower, remains within a comparable range to the CO_2 drawdown associated with rock chemical weathering in the Ecuadorian Andes and sub-Andes (2.3–4 Mg C km^{-2} yr^{-1} (ref. 34)). Basalt weathering is recognised as the primary mechanism by which volcanic activity generates a strong CO_2 sink, accounting for ~49 Tg C yr^{-1}, or 30–35% of the flux derived from continental silicate weathering[35]. Notably, organic C sequestration in tephra-buried soils in Ecuador alone represents up to ~23% of the CO_2 consumption flux from basalt weathering. Given the extensive distribution of volcanic soils in continental arc systems with explosive volcanism, such as the Cascades, Central America, the Andes and Kamchatka, this contribution is likely much greater at a global scale. In volcanic island arcs, a variable proportion of tephra emissions from explosive activity is deposited offshore, thereby reducing the potential for organic C preservation through soil burial. Nonetheless, explosive eruptions in these regions can still result in significant SOC sequestration, as suggested by the high C_{SOC} observed in multi-layered volcanic soils in Japan[36,37] and New Zealand[38,39]. We suggest that, over millennial timescales, soil burial by tephra worldwide may constitute a C sink as efficient as basalt weathering. However, while inorganic C derived from silicate weathering is transported to the oceans and effectively removed from terrestrial cycling for over 10^8 years[40], the sequestration of SOC in volcanic soils occurs over shorter timescales, typically spanning 10^3–10^4 years[5,7,11,12].

Except for the most restrictive modelling scenarios (e.g., thick tephra deposit with high probability of deposit formation, or low percentile in the SOC accumulation rate-time relationship), our estimates (Fig. 3) highlight that the SOC stock buried by tephra fallout during the Holocene dominantly exceeds, by a factor of ~3–15, the cumulative magmatic C emissions (0.08–0.4 Pg C) from all VEI ≥ 4 events in our synthetic catalogues of Ecuadorian eruptions (Methods). While likely minor compared to C storage in volcanic soils developing over a few thousand years[40], atmospheric CO_2 consumption during tephra weathering would further contribute to the C sink. Our findings lead to the counterintuitive conclusion that Holocene explosive eruptions of VEI ≥ 4 in Ecuador, through repeated burial of organic C in volcanic soils, average to C-negative events. This result stands in sharp contrast to the prevailing view that explosive volcanic activity is a net source of C emissions to the atmosphere[41–43].

Our modelling framework provides a spatially and temporally explicit estimate of the capacity of explosive eruptions to store organic C in volcanic soils and can be used to assess the C balance of explosive volcanism. It can be readily applied to other volcanic arc regions to better constrain SOC storage in the subsurface soils, thereby helping improve understanding of the role of volcanic activity in the terrestrial C cycle.

Methods

SOC stock buried by the N6 tephra from Atacazo-Ninahuilca

We sampled 35 volcanic soil outcrops around Atacazo-Ninahuilca volcano in 2016 and 2017. The outcrops were located within the 10-cm isopach of the tephra fallout from the 2,270 BP N6 eruption (Fig. 2). All outcrops contain the N5 and N6 tephra layers and a buried soil intercalated between them. The locations and altitudes of the 35 outcrops and the main properties measured for the surface and tephra-buried soils are provided in Supplementary Table 1. At each sampling site, we measured the thickness of the buried soil, i.e. the soil intercalated between the N5 and N6 tephra fallout from the 4,400 BP and 2,270 BP eruptions of Atacazo-Ninahuilca volcano[16] (Fig. 2). Approximately

100 g of material from the surface and tephra-buried soils were collected using a 7-cm soil corer. A soil sample was obtained by compositing three individual samples collected at different soil depths. For the buried soil, the soil corer was inserted at least 1-m deep horizontally. In doing so, we ensured as much as possible that the sample corresponded to a soil material that had remained isolated from the atmosphere after burial by tephra. The samples were stored in sealed plastic bags at 4 °C, then air dried prior to analysis. Plant roots and micro fauna were removed manually before sieving through a 2-mm mesh. The <2 mm soil fraction was homogenised by milling with a vibratory disk mill (Retsch RS200).

The bulk density (D_{b_soil}, in g cm^{-3}) of the tephra-buried soils was estimated from triplicates of 100 cm^3 Kopecky ring samples[44]. The coarse material fraction (solid material > 2 mm, CF, in weight %) present in the soil was separated and weighed. In general, the CF in the soil buried under the N6 tephra is low (<1%) but increases (up to 10%) in outcrops located closer to the volcano. Volcanic soils usually have acidic pH values[2] and carbonates are absent within them. Thus, the C present in our soils is composed entirely of organic C. The total C content (C_{SOC} in weight % dry soil) in the surface and tephra-buried soil samples was measured by dry combustion with an elemental analyser (Elementar Vario MACRO Cube, precision <0.1%).

For each of the 35 soil outcrops, we calculated the SOC density (d_{SOC} in kg C m^{-2}) in the N6 tephra-buried soils as follows:

$$d_{SOC} = \frac{C_{SOC}}{100} \times 1000 \times D_{b\_soil} \times z \times \frac{(1 - CF)}{100} \quad (1)$$

where z (in m) is the soil thickness.

We related the variations in d_{SOC} to altitude using a linear regression model (Supplementary Fig. 1). This allowed us to predict a d_{SOC} value for each grid cell within the ~790 km^2 area delineated by the 40 cm-isopach of the N6 tephra (Fig. 1). The SOC stock (in Tg) in the buried soils was then computed as:

$$\text{SOC stock} = \sum_{i=1}^{n} d_{SOC,i} \times A_{cell} \quad (2)$$

where n is the total number of grid cells (n = 878,014) and A_{cell} the surface area of a cell (A_{cell} = 900 m^2).

Magma volume of Atacazo-Ninahuilca's N6 eruption

The estimate of the magma volume released by an explosive eruption can be constrained by determining the volume of tephra fallout deposit associated with it[44]. This is obtained from field reconstructions that rely on the integration of isopach maps, i.e. hand-drawn contours representing equal deposit thickness, inferred from punctual observations at the outcrop level. Typically, for most Holocene eruptions, only the medial part of the tephra deposit is preserved in the landscape. To account for the missing contribution of distal tephra fallout to the total deposit volume, the thinning of the tephra deposit with distance from the volcanic vent must be described mathematically. For the N6 eruption of Atacazo-Ninahuilca, ref. 16 applied an exponential method and estimated a total volume of tephra fallout of 1.3 km^3, to which an additional 0.8 km^3 of pyroclastic density current (PDC) material was added. However, the exponential method is known to underestimate the volume of tephra deposits for which only the medial part is preserved[45]. As an alternative, we recomputed the tephra fallout volume of the N6 eruption with a power-law model[45] to extrapolate the thinning trend to missing parts of the deposit. Using a conservative distal integration limit of 300 km ± 50% and incorporating an uncertainty of 20% on both tephra thickness and isopach area, a stochastic estimation of the tephra volume[24] results in a median value of 5.0 km^3 (3.9–6.5 km^3 for the 10–90th percentiles), or 5.8 km^3 (4.7–7.3 km^3) when accounting for the PDC volume. Assuming a bulk density of 1100 kg m^{-3} for tephra deposits[46] and a density of ~2500 kg m^{-3} for a dacitic magma[47] such as that involved in the N6 eruption[16], the estimated median volume of erupted magma is ~2.6 km^3 (2.1–3.2 km^3).

Magmatic CO_2 emission from Atacazo-Ninahuilca's N6 eruption

Explosive volcanic eruptions release substantial quantities of CO_2 into the atmosphere[41–43]. These emissions originate from degassing of C originally dissolved in the magma. The paroxysmal phase of the 1991 eruption of Mt. Pinatubo, Philippines, emitted 10 Tg of CO_2 per km^3 of magma[42]. A similar rate of magmatic CO_2 degassing was used for estimating the CO_2 output of the eruptions of Tambora 1815 and Krakatau 1883 in Indonesia, Rabaul 1994 in Papua New Guinea, as well as Bishop Tuff, Katmai-Novarupta 1912; Mt. St. Helens 1980 and Redoubt 1989-1990 in the USA (refs. 41,48). This rate is considered representative of paroxysmal phases of andesitic, dacitic and rhyolitic explosive eruptions[41]. The CO_2 emissions during an explosive eruption can also be inferred by considering a primary silicate melt with a typical CO_2 content ranging from 0.2 to 0.4 weight % (refs. 49,50) and a 50% crystallisation rate during magma differentiation. Such conditions will lead to a CO_2 content in the residual melt in the range of 0.4–0.8 weight % and therefore, 1 km^3 of magma with 50% crystals by volume will contain 1.3 Tg of melt (assuming a density of ~2500 kg m^{-3} (ref. 46)) and approximately 5–10 Tg of CO_2. Assuming complete CO_2 release from the magma during an explosive eruption, a conservative estimate for the magmatic CO_2 degassing rate (F_{CO2}) is 10 Tg km^{-3}, an estimate fully consistent with field-based measurements[41,42,48].

Knowing the magma volume (V_{magma}) of an explosive eruption (see above), the corresponding mass of magmatic C emitted (M_C, in Tg) is calculated using:

$$M_C = V_{magma} \times F_{CO2} \times \frac{m_C}{m_{CO2}} \quad (3)$$

where m_C and m_{CO2} are the molar masses of C and CO_2, respectively, and F_{CO2} = 10 Tg km^{-3}. Applying equation [3] to the N6 eruption of Atacazo-Ninahuilca indicates that 5.7–8.7 Tg (median = 7.2 Tg) of magmatic C were released into the atmosphere.

Frequency of Holocene explosive eruptions in Ecuador

We focused our study on eruptions with a VEI of 4, 5 and 6, which are sub-Plinian/Plinian events producing tephra volumes ranging from 0.1 to 100 km^3 (ref. 15). Eruptions with a lower VEI are disregarded because the spatial dispersion of their tephra is limited, are either underreported[23] or missing[51] from existing databases, and may feature a variety of eruption dynamics that do not necessarily follow the relationship between magma volume and CO_2 emission used in this study (see above). We used the Global Volcanism Program (GVP)[23] database to infer the eruptive history of all Andean Ecuadorian volcanoes during the Holocene. The database records 42 eruptions ≥ VEI 4 from a total of ten volcanoes, including 27 VEI 4 (65%), 14 VEI 5 (33%) and one VEI 6 (2%) eruptions (Supplementary Table 3). Cotopaxi volcano dominates the eruptive record, with 14 eruptions of VEI 4 and 7 eruptions of VEI 5. Only Quilotoa volcano produced a VEI 6 eruption.

Under the assumption that eruptions of VEI ≥ 4 are independent events[52,53], we estimated a monthly average recurrence interval (ARI) over the Holocene. The monthly ARI (Supplementary Table 3) was computed as the number of eruptions of a given VEI normalised by the time period over which the eruption record is complete (i.e. 520 years for VEI 4 and 12,020 years for VEI 5 and 6). Supplementary Fig. 5 shows the cumulative number of eruptions recorded in the GVP catalogue for the ten selected Ecuadorian volcanoes. Since the record completeness varies with eruption magnitude[53], the eruption frequency obtained from the GVP catalogue must be interpreted with care. Following previous studies[52,53], we assumed that the catalogue of VEI 4 eruptions

is only complete after 1500 AD and estimated an ARI for the ten volcanoes in continental Ecuador of 1.62×10^{-3} VEI 4 eruptions per month. However, there was a transition from rhyolitic to andesitic volcanism ~4000 years ago[54], after which only one VEI 5 eruption is recorded. Evidence for such changes in eruptive dynamics led us to adopt a conservative approach: we considered the catalogue of VEI 5 eruptions as complete and estimated an ARI of 9.71×10^{-5} VEI 5 eruptions per month. Finally, we included only one eruption of VEI 6 for the Holocene, resulting in an ARI of 6.93×10^{-6} VEI 6 eruptions per month.

Using the ARI values, we generated 1,000 synthetic eruption catalogues spanning the Holocene. The stochastic sampling procedure was performed in Python 3.9 with the random.choices() function. Firstly, we sampled whether an eruption of any of VEI 4, 5 or 6 occurred over the 144,240 monthly time steps between the beginning of the Holocene and 2020 using the sum of the total ARI for each VEI. Secondly, for time steps when an eruption occurred, we used the total ARI of each VEI as relative weights to sample the VEI of the eruption. Thirdly, with sampled VEI, we used the ARI of each volcano as relative weights to sample a volcano source. Supplementary Fig. 6 summarises the distributions of eruptions of all VEI sampled over the 1,000 synthetic eruption catalogues. On average, each catalogue contains 248 eruptions (ranging from 200 to 309), with most of the discrepancy between the observed 42 eruptions in the GVP database attributed to under-representation of VEI 4 eruptions.

Spatial extent of tephra deposits from VEI ≥ 4 eruptions in Ecuador

The spatial distribution of tephra fallout resulting from VEI ≥ 4 explosive eruptions was estimated using a scenario-based probabilistic approach[55]. We modelled three eruption scenarios of VEI 4, 5 and 6 using Atacazo-Ninahuilca volcano as a source with the Tephra2 advection-diffusion model within the TephraProb probabilistic framework[24]. Each scenario consists of 5,000 runs of Tephra2, where each run samples a set of eruption source parameters (ESPs; Supplementary Table 4) and a wind condition stochastically. Wind conditions for Ecuador were obtained from the ERA5 database from the European Centre for Medium-Range Weather Forecasts[56], using 16 years of four-daily data from 2000 to 2015 (Supplementary Fig. 3). Outputs were compiled into probabilistic isomass maps, which show the spatial distribution of tephra fallout accumulation associated with a specific exceedance probability. For instance, for a given VEI and a given spatial coordinate, a tephra accumulation of 10 kg m^{-2} at a 25% probability threshold implies that a deposit ≥ 10 kg m^{-2} was obtained in 1250 of the 5000 simulations.

Magmatic CO_2 emissions from VEI ≥ 4 Holocene eruptions in Ecuador

Similar to the approach discussed above for the N6 eruption of Atacazo-Ninahuilca, the mass of CO_2 emitted by an explosive eruption is obtained by considering a degassing rate of 10 Tg CO_2 per km^3 of magma erupted. For each of the 5000 sets of ESPs sampled for each VEI value in the probabilistic modelling, we converted the tephra volume (V_{tephra}) into a mass of magmatic C emitted (M_C, in Tg) using:

$$M_C = V_{tephra} \times \frac{D_{b\_tephra}}{D_{magma}} \times 10 \times \frac{m_C}{m_{CO2}} \quad (4)$$

where D_{b_tephra} is the tephra deposit bulk density (1100 kg m^{-3} (ref. 46)), D_{magma} is the magma density (2500 kg m^{-3} (ref. 47)), m_C is the molar mass of C and m_{CO2} is the molar mass of CO_2. For a given VEI, we express the 10th, 50th and 90th percentiles of M_C.

Spatio-temporal evolution of Holocene tephra deposits in Ecuador

Following the methodology described above, every synthetic eruption catalogue records if an eruption occurs at each time step and, when it does, the corresponding VEI and source volcano are identified. Conceptually, the spatio-temporal reconstruction of tephra accumulation over the Holocene in the Ecuadorian Andes can be schematised as a three-dimensional matrix of coordinates [y, x, t], with a spatial domain at a 1 km resolution and a temporal domain at a monthly resolution. At every time step of each synthetic eruption catalogue where an eruption occurs, the tephra accumulation modelled for Atacazo-Ninahuilca volcano for the relevant VEI is spatially translated to the source volcano and stored in the three-dimensional matrix.

The translation of tephra accumulations modelled for a VEI 4-, 5- or 6-eruption of Atacazo-Ninahuilca volcano to other volcanoes in the region can be justified as follows. Firstly, from a computation perspective, modelling each eruption (average of 248 eruptions per catalogue) for each catalogue (n = 1000) in a probabilistic way would require 1.24×10^9 individual runs of the Tephra2 model with TephraProb[24]. Our approach reduces this to a more manageable 15,000 simulations. Secondly, Tephra2 relies on an analytical solution of advection-diffusion equation, which significantly decreases computation time compared to numerical models, and also allows probabilistic modelling. Since no local topographic effect on ground tephra accumulation can be resolved by Tephra2, we used a 1 km spaced computation grid set at a constant elevation of 2500 m above sea level, which we assume to be representative for all volcanoes in Ecuador. Finally, Tephra2 works with two-dimensional wind profiles. Existing analyses of wind data over Ecuador[57] suggest that the Andean arc experiences similar general wind patterns with a dominant westward direction. Since i) we consider the general wind direction to be of first order importance in our study compared to small-scale orographic wind effects and ii) general wind directions inferred from the ERA5 database[56] are similar along a north-south profile across Ecuadorian volcanoes (Supplementary Fig. 3), we assumed wind conditions at Atacazo-Ninahuilca volcano to be representative for the studied region.

SOC accumulation rate in volcanic soils

In general, climatic conditions, namely temperature and precipitation, are key drivers of SOC accumulation, affecting both C input into the soil and SOC decomposition[17,18]. Parent material also influences SOC accumulation due to its control on soil mineralogy, texture and fertility, which affect net primary productivity and the stabilisation of organic matter[18,58,59]. At the regional and continental scales in various climatic zones, vegetation type is another factor that modulates SOC storage. Volcanic soils have a large potential for retaining organic C[1,2]. This is due to abundant reactive surfaces, the formation of organo-mineral associations and the development of microaggregation which protect SOC from decomposition and enhance its residence time.

To describe the rate of organic C accumulation (in g m^{-2} yr^{-1}) in volcanic soils of different age, we revisited a previous study[12] by adding measurements, including our own samples of volcanic soils collected in the Ecuadorian Andes (Supplementary Table 5). The revised dataset includes 76 measurements covering volcanic soils of varying age (-70 to 16,000 yr), formed from parent material composition ranging from basalt to rhyolite and located in contrasted climate zones (polar to tropical equatorial). As shown in Supplementary Fig. 4, the relationship between SOC accumulation rate and soil age in volcanic soils can be described by a power function. The decrease in the rate of SOC accumulation over time is attributed to changes in reactive iron- and aluminium-bearing soil constituents, which result in a reduced efficiency of organic matter stabilisation[25,26]. We used quantile regression to estimate prediction intervals based on the 10th, 50th and 90th percentiles.

Ethics and inclusion statement

The field study in the Atacazo region in Ecuador was conducted with consideration of ethical and inclusive research practices. While local researchers were not directly involved as co-authors, we sought advice

from Ecuadorian volcanologists regarding sampling site selection and site access. We acknowledge the contribution of local researchers, whose published data provided insights that guided our selection of sampling locations. Their work is duly cited.

Data availability

All source data are available in the Supplementary Information.

Code availability

The numerical model used for estimating the C balance of explosive eruptions in a volcanically active region over time was developed in Python v.3.11. The code is available on GitHub: https://doi.org/10.5281/zenodo.10958530.

References

1. Batjes, N. H. Total carbon and nitrogen in the soils of the world. *Eur. J. Soil Sci.* **65**, 10–21 (2014).
2. Dahlgren, R. A., Saigusa, M. & Ugolini, F. C. The nature, properties and management of volcanic soils. *Adv. Agron.* **82**, 113–182 (2004).
3. Asano, M. & Wagai, R. Evidence of aggregate hierarchy at micro- to submicron scales in an allophanic andisol. *Geoderma* **216**, 62–74 (2014).
4. Matus, F., Rumpel, C., Neculman, R., Panichini, M. & Mora, M. L. Soil carbon storage and stabilisation in andic soils: a review. *Catena* **120**, 102–110 (2014).
5. Lawrence, C. R., Harden, J. W., Xu, X., Schulz, M. S. & Trumbore, S. E. Long-term controls on soil organic carbon with depth and time: a case study from the Cowlitz River Chronosequence, WA USA. *Geoderma* **247–248**, 73–87 (2015).
6. Ugolini, F. C. & Dahlgren, R. A. Soil development in volcanic ash. *Glob. Environ. Res.* **6**, 69–81 (2002).
7. Fontaine, S. et al. Stability of organic carbon in deep soil layers controlled by fresh carbon supply. *Nature* **450**, 277–280 (2007).
8. Rumpel, C. & Kögel-Knabner, I. Deep soil organic matter—a key but poorly understood component of terrestrial C cycle. *Plant Soil* **338**, 143–158 (2011).
9. Kirschbaum, M. U. F. et al. Sequestration of soil carbon by burying it deeper within the profile: A theoretical exploration of three possible mechanisms. *Soil Biol. Biochem.* **163**, 108432 (2021).
10. Balesdent, J. et al. Atmosphere–soil carbon transfer as a function of soil depth. *Nature* **559**, 599–602 (2018).
11. Torn, M. S., Trumbore, S. E., Chadwick, O. A., Vitousek, P. M. & Hendricks, D. M. Mineral control of soil organic carbon storage and turnover. *Nature* **389**, 170–173 (1997).
12. Zehetner, F. Does organic carbon sequestration in volcanic soils offset volcanic CO_2 emissions? *Quat. Sci. Rev.* **29**, 1313–1316 (2010).
13. Chaopricha, N. T. & Marín-Spiotta, E. Soil burial contributes to deep soil organic carbon storage. *Soil Biol. Biochem.* **69**, 251–264 (2014).
14. Chadwick, O. A., Kelly, E. F., Merritts, D. M. & Amundson, R. G. Carbon dioxide consumption during soil development. *Biogeochemistry* **24**, 115–127 (1994).
15. Newhall, C. G. & Self, S. The volcanic explosivity index (VEI) an estimate of explosive magnitude for historical volcanism. *J. Geophys. Res. Oceans* **87**, 1231–1238 (1982).
16. Hidalgo, S. et al. Late Pleistocene and Holocene activity of the Atacazo–Ninahuilca Volcanic Complex (Ecuador). *J. Volcanol. Geotherm. Res.* **176**, 16–26 (2008).
17. Wiesmeier, M. et al. Soil organic carbon storage as a key function of soils - A review of drivers and indicators at various scales. *Geoderma* **333**, 149–162 (2019).
18. de Brogniez, D. et al. In *Soil Carbon* (eds Hartemink, A. E. & McSweeney, K.) 393–405, (Springer International Publishing, 2014).
19. Leifeld, J., Bassin, S. & Fuhrer, J. Carbon stocks in Swiss agricultural soils predicted by land-use, soil characteristics, and altitude. *Agric. Ecosyst. Environ.* **105**, 255–266 (2005).
20. Farr, T. G. et al. The shuttle radar topography mission. *Rev. Geophys.* **45**, RG2004 (2007).
21. Hengl, T. et al. SoilGrids250m: Global gridded soil information based on machine learning. *PLoS One* **12**, e0169748 (2017).
22. Espinosa, J., Moreno, J. & Bernal, G. The Soils of Ecuador. https://doi.org/10.1007/978-3-319-25319-0 (Springer Cham, 2018).
23. Global Volcanism Program. [Database] Volcanoes of the World (v. 5.0.4; 17 Apr 2023). Distributed by Smithsonian Institution, compiled by Venzke, E., https://doi.org/10.5479/si.GVP.VOTW5-2023.5.1 (2023).
24. Biass, S., Bonadonna, C., Connor, L. & Connor, C. TephraProb: a Matlab package for probabilistic hazard assessments of tephra fallout. *J. Appl. Volcanol.* **5**, 10 (2016).
25. Wada, K. & Aomine, S. Soil development on volcanic materials during the Quaternary. *Soil Sci.* **116**, 170–177 (1973).
26. Toma, Y. et al. Soil carbon stocks and carbon sequestration rates in seminatural grassland in Aso region, Kumamoto, Southern Japan. *Glob. Change Biol.* **19**, 1676–1687 (2013).
27. Basile-Doelsch, I. et al. Mineralogical control of organic carbon dynamics in a volcanic ash soil on La Reunion. *Eur. J. Soil Sci.* **56**, 689–703 (2005).
28. Tonneijck, F. H., van der Plicht, J., Jansen, B., Verstraten, J. M. & Hooghiemstra, H. Radiocarbon dating of soil organic matter fractions in Andosols in Northern Ecuador. *Radiocarbon* **48**, 337–353 (2006).
29. Casati, E. et al. Geo-pedological contribution to the reconstruction of Holocene activity of Chaitén volcano (Patagonia, Chile). *J. South Am. Earth Sci.* **94**, 102222 (2019).
30. Bernoux, M. & Volkoff, B. In *Carbon sequestration in soils of Latin America* (eds Lal, R. et al.) 65–75, (Haworth Press, 2006).
31. Marín-Spiotta, E. et al. Long-term stabilization of deep soil carbon by fire and burial during early Holocene climate change. *Nat. Geosci.* **7**, 428–432 (2014).
32. James, J., Devine, W., Harrison, R. & Terry, T. Deep soil carbon: quantification and modeling in subsurface layers. *Soil Sci. Soc. Am. J.* **78**, S1–S10 (2014).
33. Zech, M. et al. Buried black soils on the slopes of Mt. Kilimanjaro as a regional carbon storage hotspot. *Catena* **112**, 125–130 (2014).
34. Moquet, J.-S. et al. Chemical weathering and atmospheric/soil CO_2 uptake in the Andean and Foreland Amazon basins. *Chem. Geol.* **287**, 1–26 (2011).
35. Dessert, C., Dupré, B., Gaillardet, J., François, L. M. & Allègre, C. J. Basalt weathering laws and the impact of basalt weathering on the global carbon cycle. *Chem. Geol.* **202**, 257–273 (2003).
36. Morisada, K., Ono, K. & Kanomata, H. Organic carbon stock in forest soils in Japan. *Geoderma* **119**, 21–32 (2004).
37. Matsui, K. et al. Soil carbon and nitrogen stock of the Japanese agricultural land estimated by the national soil monitoring database (2015–2018). *Soil Sci. Plant Nutr.* **67**, 633–642 (2021).
38. Tate, K. R. et al. Organic carbon stocks in New Zealand's terrestrial ecosystems. *J. R. Soc. N. Z.* **27**, 315–335 (1997).
39. Hewitt, A. E., Balks, M. R. & Lowe, D. J. The Soils of Aotearoa New Zealand. https://doi.org/10.1007/978-3-030-64763-6 (Springer International Publishing, 2021).
40. Berner, R. A., Lasaga, A. C. & Garrels, R. M. The carbonate-silicate geochemical cycle and its effect on atmospheric carbon dioxide over the past 100 million years. *Am. J. Sci.* **283**, 641–683 (1983).
41. Burton, M. R., Sawyer, G. M. & Granieri, D. Deep carbon emissions from volcanoes. *Rev. Mineral. Geochem.* **75**, 323–354 (2013).
42. Gerlach, T. M. Present-day CO_2 emissions from volcanoes. *EOS Trans., AGU* **72**, 249–255 (1991).
43. Fischer, T. P. et al. The emissions of CO_2 and other volatiles from the world's subaerial volcanoes. *Sci. Rep.* **9**, 18716 (2019).
44. Blake, G. R. In *Methods of Soil Analysis: Part 1 Physical and Mineralogical Properties, Including Statistics of Measurement and*

Sampling Agronomy Monograph. (ed C. A. Black) Ch. 30, 374–390 (American Society of Agronomy, Inc., 1965).
45. Bonadonna, C. & Houghton, B. Total grain-size distribution and volume of tephra-fall deposits. *Bull. Volcanol.* **67**, 441–456 (2005).
46. Paladio-Melosantos, M. et al. In *Fire and Mud: Eruptions and Lahars of Mount Pinatubo, Philippines* (eds. Newhall, C. G. & Punongbayan, R. S.) 513–535 (University of Washington Press, 1996).
47. Iacovino, K. & Till, C. B. DensityX: A program for calculating the densities of magmatic liquids up to 1,627 °C and 30 kbar. *Volcanica* **2**, 1–10 (2019).
48. Wallace, P. J. In *Developments in Volcanology* (eds Bodnar, B. J. & DeVivo, B.) 105–127, (Elsevier, 2003).
49. Holloway, J. R. & Blank, J. G. In *Volatiles in Magmas* (eds Michael, R. C. & John, R. H.) 187–230, (De Gruyter, 1994).
50. Wallace, P. J. Volatiles in subduction zone magmas: concentrations and fluxes based on melt inclusion and volcanic gas data. *J. Volcanol. Geotherm. Res.* **140**, 217–240 (2005).
51. Crosweller, H. S. et al. Global database on large magnitude explosive volcanic eruptions (LaMEVE). *J. Appl. Volcanol.* **1**, 1–13 (2012).
52. Dzierma, Y. & Wehrmann, H. Statistical eruption forecast for the Chilean Southern Volcanic Zone: typical probabilities of volcanic eruptions as baseline for possibly enhanced activity following the large 2010 Concepción earthquake. *Nat. Hazards Earth Syst. Sci.* **10**, 2093–2108 (2010).
53. Deligne, N. I., Coles, S. G. & Sparks, R. S. J. Recurrence rates of large explosive volcanic eruptions. *J. Geophys. Res. Solid Earth* **115**, https://doi.org/10.1029/2009jb006554 (2010).
54. Hall, M. & Mothes, P. The rhyolitic–andesitic eruptive history of Cotopaxi volcano, Ecuador. *Bull. Volcanol.* **70**, 675–702 (2008).
55. Bonadonna, C. In *Statistics in Volcanology* Vol. 1 (eds H. M. Mader, S. G. Coles, C. B. Connor, & L. J. Connor) 243–259, (Geological Society of London, 2006).
56. Hersbach, H. et al. The ERA5 global reanalysis. *Q. J. R. Meteorol. Soc.* **146**, 1999–2049 (2020).
57. Volentik, A. C. M. & Houghton, B. F. Tephra fallout hazards at Quito International Airport (Ecuador). *Bull. Volcanol.* **77**, 50 (2015).
58. Herold, N. et al. Controls on soil carbon storage and turnover in German landscapes. *Biogeochemistry* **119**, 435–451 (2014).
59. Gray, J. M., Bishop, T. F. A. & Wilson, B. R. Factors controlling soil organic carbon stocks with depth in eastern Australia. *Soil Sci. Soc. Am. J.* **79**, 1741–1751 (2016).

Acknowledgements

We are grateful to S. Hidalgo (Instituto Geofísico, Escuela Politécnica Nacional (IG-EPN)) for generously sharing her dataset on the N5 and N6 tephra fallout distribution. We also thank Patty Mothes (IG-EPN) for her insightful discussions and encouragement. We appreciate the valuable discussions with K. Van Oost and C. Chenu, as well as thoughtful comments from E. Maters and D. Henley on an earlier draft. M.P. acknowledges funding from FNRS–FRIA (FC 9756).

Author contributions

P.D. and S.B. designed the study. P.D., S.B., M.P. and B.L. undertook model development. S.B., M.P. and B.L. performed model simulations and coding. P.D. and M.P. conducted the soil sampling in Ecuador and the laboratory analyses. P.D., S.B., M.P. and B.L. undertook data analysis and synthesis. P.D. and S.B. wrote the manuscript with input from co-authors.

Competing interests

The authors declare no competing interests.

Additional information

Supplementary information The online version contains supplementary material available at https://doi.org/10.1038/s41467-025-59692-4.

Correspondence and requests for materials should be addressed to Pierre Delmelle.

Peer review information *Nature Communications* thanks Mike Widdowson and the other anonymous reviewer(s) for their contribution to the peer review of this work. A peer review file is available.